THE JOURNAL OF BIOLOGICAL CHEMISTRY
Vol. 277, No. 9, Issue of March 1, pp. 7369–7376, 2002
Printed in U.S.A.

Probing the Conformational Change of *Escherichia coli* Undecaprenyl Pyrophosphate Synthase during Catalysis Using an Inhibitor and Tryptophan Mutants*

Received for publication, October 17, 2001, and in revised form, December 10, 2001
Published, JBC Papers in Press, December 14, 2001, DOI 10.1074/jbc.M110014200

Yi-Hung Chen‡§¶, Annie P.-C. Chen¶‖, Chao-Tsen Chen§, Andrew H.-J. Wang‡‖, and Po-Huang Liang‡‖**

From the ‡Institute of Biological Chemistry, Academia Sinica, Taipei 11529 and ‖Institute of Biochemical Sciences and §Department of Chemistry, National Taiwan University, Taipei 10098, Taiwan

Undecaprenyl pyrophosphate synthase (UPPS) catalyzes the consecutive condensation reactions of eight isopentenyl pyrophosphate (IPP) with farnesyl pyrophosphate (FPP) to generate C_{55} undecaprenyl pyrophosphate (UPP). In the present study, site-directed mutagenesis, fluorescence quenching, and stopped-flow methods were utilized to examine the substrate binding and the protein conformational change. (*S*)-Farnesyl thiopyrophosphate (FsPP), a FPP analogue, was synthesized to probe the enzyme inhibition and events associated with the protein fluorescence change. This compound with a much less labile thiopyrophosphate shows K_i value of 0.2 μM in the inhibition of *Escherichia coli* UPPS and serves as a poor substrate, with the k_{cat} value (3.1×10^{-7} s^{-1}) 10^7 times smaller than using FPP as the substrate. Reduction of protein intrinsic fluorescence was observed upon addition of FPP (or FsPP) to the UPPS solution. Moreover, fluorescence studies carried out using W91F and other mutant UPPS with Trp replaced by Phe indicate that FPP binding mainly quenches the fluorescence of Trp-91, a residue in the α3 helix that moves toward the active site during substrate binding. Using stopped-flow apparatus, a three-phase protein fluorescence change with time was observed by mixing the E·FPP complex with IPP in the presence of Mg^{2+}. However, during the binding of E·FsPP with IPP, only the fastest phase was observed. These results suggest that the first phase is due to the IPP binding to E·FPP complex, and the other two slow phases are originated from the protein conformational change. The two slow phases coincide with the time course of FPP chain elongation from C_{15} to C_{55} and product release.

Undecaprenyl pyrophosphate synthase (UPPS)[1] catalyzes the chain elongation of farnesyl pyrophosphate (FPP) with eight molecules of isopentenyl pyrophosphate (IPP) to generate C_{55} undecaprenyl pyrophosphate (UPP) (1–4). It belongs to a *cis*-prenyltransferase family and shows sequence homology with other members including dehydrodolichyl pyrophosphate synthase from yeast (5), a C_{15} and a C_{50} isopentenyl pyrophosphate synthases found in *Mycobacterium tuberculosis* (6), and a C_{120} prenyltransferase from *Arabidopsis thaliana* (7). The biological function of bacterial UPP is to serve as a carrier to transport UDP-*N*-acetylmuramic acid pentapeptide, which subsequently reacts with UDP-*N*-acetylglucosamine to form lipid II, to extracellular compartments where lipid II molecules are assembled into peptidoglycans of the cell wall (8, 9). The enzyme is essential for bacterial survival due to its vital role in cell wall biosynthesis (10). The crystal structures of UPPS from *Micrococcus luteus* and *Escherichia coli* solved, respectively, by Fujihashi *et al.* (11) and by Ko *et al.* (12) are the first two structures in the *cis*-prenyltransferase family. In *E. coli* UPPS structure, an elongated tunnel with the hydrophobic amino acid side chains covering the entire interior surface was proposed to accommodate the UPP product (Fig. 1*A*) (12). This hydrophobic tunnel is surrounded by two α-helices (α2 and α3) and four β-strands (βA-βB-βD-βC). On the top portion of the tunnel, several conserved hydrophilic amino acids in the vicinity of Asp-26 including Asn-28, Arg-30, His-43, Phe-70, Ser-71, Arg-194, Glu-198, and Arg-200 in subunit A as well as the Glu-213 from subunit B of the UPPS homodimer are proposed to involve in the FPP and IPP binding. Site-directed mutagenesis studies suggest that IPP is probably bound to the area of Glu-213, Arg-194, and Arg-200 since mutations of these residues to Ala resulted in significantly increased IPP K_m and decreased k_{cat} values (13–15). FPP is proposed to bind with its pyrophosphate group near the Asp-26, Asn-28, Arg-30, and Glu-198 area and its C_{15}-tail pointing toward the bottom of the active site (11, 12, 14, 15).

A disordered loop consisting of the amino acid residues 72–83 is proposed to bring the IPP to a correct position and orientation relative to FPP, needed to initiate the condensation reaction (12). The replacement of Trp-75 residue, located in the loop with Ala, increases the FPP and IPP K_m values, indicating that Trp-75 is close to the bound IPP and FPP (12, 15). The mutations of several other residues such as N74A, E81A, and R77A of the loop display decreased k_{cat} and increased IPP K_m values (12). The loop may also serve as a hinge for the necessary protein conformational change in catalysis since two conformers observed in the *E. coli* UPPS structure differ in the position of α3 helix (Fig. 1*A*), which is connected to the loop (12). In the closed conformer, the tunnel is narrow within which an elongated electron density envelope (probably Triton or polyethylene glycol used in the crystallization) is visible. On the other hand, the open form of the tunnel contains only water molecules in the active site area. This loop is proposed to

* This work was supported by Academia Sinica and by National Science Council Grant NSC90-2113-M-001-063 (to P.-H. L.). The costs of publication of this article were defrayed in part by the payment of page charges. This article must therefore be hereby marked "*advertisement*" in accordance with 18 U.S.C. Section 1734 solely to indicate this fact.

¶ These authors have equal contribution.
** To whom correspondence should be addressed. Tel.: 886-2-2785-5696 (Ext. 6070); Fax: 886-2-2788-9759; E-mail: phliang@gate.sinica.edu.tw.

[1] The abbreviations used are: UPPS, undecaprenyl pyrophosphate (UPP) synthase; FPP, farnesyl pyrophosphate; FsPP, (*S*)-farnesyl thiopyrophosphate; IPP, isopentenyl pyrophosphate; HPLC, high performance liquid chromatography.

function in bringing the α3 helix close to α2, leading to the formation of the closed form, in which the enzyme has better interactions with the substrate.

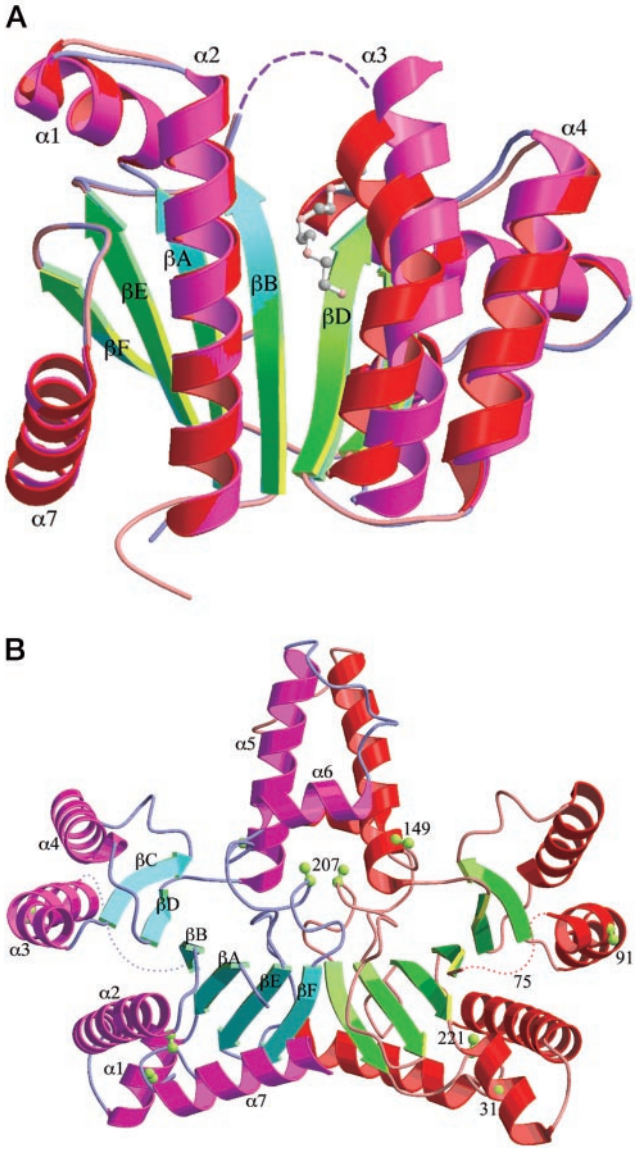

FIG. 1. *A*, the hydrophobic tunnel surrounded by two α-helices and four β-strands with a flexible loop connecting α3 and βB. The α3 helix in the open conformer is shown in *magenta*, and in the closed form is shown in *red*. Upon binding of FPP, the flexible loop as well as α3 might move toward the active site, and the fluorescence of Trp-91 located in α3 is changed. The figure is adopted from our previous paper (12). *B*, ribbon structure of the UPPS dimer with six Trp residues shown as *green dots* and *numbered* in subunit A. This is an orthogonal view with the dyad lying horizontal. The seven α-helices and six β-strands are shown in *red* and *green* for subunit A and in *magenta* and *cyan* for subunit B. The figure is prepared using MolScript (22).

In the present study, fluorescence experiments were utilized to examine the binding of FPP and IPP since the binding of substrate to enzyme may alter the UPPS intrinsic fluorescence. All Trp residues including Trp-31, Trp-75, Trp-91, Trp-149, Trp-207, and Trp-221 in the *E. coli* UPPS primary sequence were individually mutated to Phe for the fluorescence studies (see Fig. 1*B* for the positions of Trp residues in the UPPS). Furthermore, stopped-flow fluorescence technology was employed to monitor the protein conformational change associated with UPPS catalysis. To serve the above purposes as well as to test the inhibition of the enzyme, (*S*)-farnesyl thiopyrophosphate (FsPP, a FPP analogue) was synthesized. Due to its much less labile thiopyrophosphate group and its structural similarity to FPP, FsPP could act as a good UPPS inhibitor. Previously, the thiol analogue of geranyl pyrophosphate was prepared and used as an inhibitor as well as an alternative substrate for farnesyl pyrophosphate synthase, which synthesizes FPP from geranyl pyrophosphate and IPP (16). The geranyl thiopyrophosphate was an extremely poor substrate for farnesyl pyrophosphate synthase and showed 10^6 lower activity compared with the normal substrate (16). However, FPP thiol analogue has not been tested as an inhibitor for the enzymes catalyzing FPP chain elongation until now. The results of inhibition of UPPS by FsPP and the fluorescence binding and stopped-flow experiments using FPP or its thiol analogue to identify the protein conformational change are presented in this paper.

EXPERIMENTAL PROCEDURES

Reagents and General Methods—Trimethylphosphate, tetra-*n*-butylammonium hydroxide, dimethylchlorothiophosphate, iodotrimethylsilane, and all-*trans*-farnesyl chloride were purchased from Aldrich. Dowex AG50 × 8 ion exchange column (NH_4^+ form) was obtained from Sigma. The radiolabeled [^{14}C]IPP (55 mCi/mmol) was purchased from Amersham Biosciences, Inc. The all-*trans*-FPP and IPP were obtained from Sigma. Reversed-phase thin-layer chromatography (TLC) plate was the product of Merck. *Taq* DNA polymerase was purchased from Invitrogen. The plasmid mini-prep kit, DNA gel extraction kit, and nickel nitrilotriacetic acid resin were obtained from Qiagen. Potato acidic phosphatase (2 units/mg) was purchased from Roche Molecular Biochemicals. The protein expression kit including the pET32Xa/LIC vector and competent JM109 and BL21 cells and Factor Xa protease were obtained from Novagen. The mutagenic primers were prepared by MDBio Co. All commercial buffers and reagents were of the highest grade.

NMR measurements were performed using Bruker AVANCE spectrometer. Mass analysis was carried out using Jeol-SX102A instrument. For HPLC chromatography, a Waters system with a reverse phase Hypersil® HS C8 column (250 × 4.6 mm) obtained from ThermoQuest was used.

Preparation of (S)-Farnesyl Thiopyrophosphate—Synthesis of (*S*)-farnesyl thiopyrophosphate was performed using the procedures previously reported for preparing geranyl thiopyrophosphate via the synthesis of tetra-*n*-butylammonium dimethylphosphate and tetramethyl thiopyrophosphate (16) with modification in making (*S*)-farnesyl thiopyrophosphate from tetramethyl thiopyrophosphate as described below.

Tetramethyl thiopyrophosphate (0.5 g, 2.0 mmol) was added dropwise to iodotrimethylsilane (2.26 g, 11.28 mmol) at −35 °C, and the solution was allowed to warm to room temperature over 6 h. The

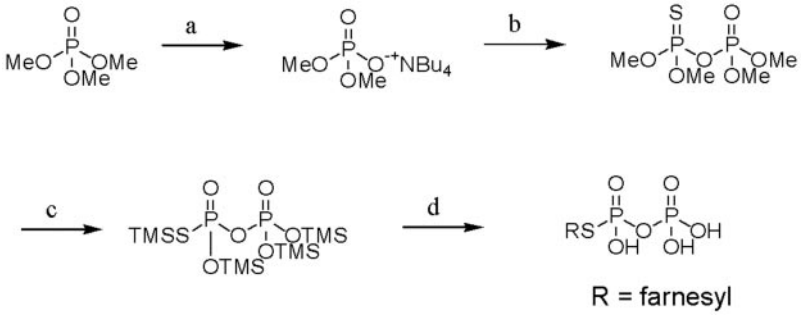

SCHEME 1. **Synthesis of (*S*)-farnesyl thiopyrophosphate.** The reaction conditions are tetra-*n*-butylammonium hydroxide (NBu_4)), 100 °C, 24 h, 95% (*a*), $(OMe)_2P(S)Cl$, CH_3CN, −35 °C, 30 min, 35% (*b*), trimethylsilane (*TMS*), −35 °C → room temperature, 6 h, 97% (c), and tetra-*n*-butylammonium hydroxide/H_2O, farnesyl chloride (*d*).

mixture was concentrated under reduced pressure to afford brown semi-solid residue. The residue was then dissolved in 7 ml of acetonitrile, adjusted to pH 6 with 40% (w/w) aqueous tetra-*n*-butylammonium hydroxide, and further titrated with 0.4 M aqueous tetra-*n*-butylammonium hydroxide to pH 7–7.2. The organic solvent was first removed by vacuum, and the remaining solution was lyophilized to give the substance for the next step without further purification. All-*trans*-farnesyl chloride (220 mg, 0.9 mmol) was added dropwise to the *tris*-(trimethylsilane) thiopyrophosphate solution at 25 °C, and the mixture was stirred at room temperature for 8 h. The organic solvent was removed by a rotatory evaporator to afford a brown solid. The solid was dissolved in a limited amount of deionized water and passed through a short Dowex 50 × 8 ion exchange column (NH_4^+ form). The collected filtrate was lyophilized to yield a white solid. This solid was further purified by reversed-phase HPLC using a program of 5 min of 100% A followed by a linear gradient of 100% A to 100% B over 30 min with a flow rate of 1 ml/min (A, 25 mM aqueous ammonium bicarbonate (pH 8.0); B, acetonitrile). The fractions containing product were collected and lyophilized to afford 239 mg of white solid (70% yield): ^{1}H NMR (400 MHz, D_2O) δ 1.62 (6H, s, CH_3), 1.69 (3H, s, CH_3), 1.71 (3H, s, CH_3), 2.00–2.15 (8H, m, CH_2), 3.53 (2H, t, J = 8.4 Hz), 5.19 (2H, m, CH), 5.42 (1H, t, J = 8 Hz); ^{13}C NMR (100 MHz, D_2O) δ 15.24, 16.92, 24.80, 25.55, 25.72, 27.94 (d), 38.72, 119.89(d), 124.22, 124.43, 133.49, 136.61, 140.77; ^{31}P NMR (D_2O) δ −7.47 (d), 7.78 (d); high resolution mass (fast atom bombardment) calculated for $C_{15}H_{28}O_6P_2S$ 398.1082, found $[M-1]^-$ m/z = 397.1008.

Measurement of IC_{50} for (S)-Farnesyl Thiopyrophosphate—The measurement of the inhibition constant for FsPP analogue was performed in a reaction mixture containing 0.03 μM UPPS, 3 μM FPP, and 50 μM [^{14}C]IPP in a buffer of 100 mM Hepes-KOH (pH 7.5), 50 mM KCl, 0.5 mM $MgCl_2$, and 0.1% Triton X-100 in the presence of various concentrations of inhibitor ranged from 0 to 6 μM. The 0.1% Triton X-100 was included in the reaction so that the product release did not limit the reaction so as to allow the measurement of IPP condensation rate at each inhibitor concentration. Portions of reaction mixture periodically withdrawn were mixed with 10 mM EDTA to terminate the reaction, and 1-butanol was utilized to extract the enzyme products for quantification using scintillation counting. The initial rate was obtained for zero and different concentrations of inhibitor, and the IC_{50} value of the inhibitor was determined by fitting the reaction rate *versus* inhibitor concentration using the following equations (17).

$$A\ (\mathrm{I}) = A\ (0) \times \{1 - [I/(I + K_i(1 + S/K_m))]\} \quad \text{(Eq. 1)}$$

$$\mathrm{IC}_{50} = K_i(1 + S/K_m) \quad \text{(Eq. 2)}$$

In these equations, A (I) is the enzyme activity with inhibitor concentration I, A (0) is enzyme activity without inhibitor, I is the inhibitor concentration, K_i is the inhibition constant of inhibitor, S is the FPP concentration, and K_m is Michaelis constant of FPP.

Test of FsPP as an Alternative Substrate of UPPS—In a reaction mixture containing 0.1 μM UPPS, 50 μM [^{14}C]IPP, 0.5 mM $MgCl_2$, 50 mM KCl, and 0.1% Triton X-100 in 100 mM Hepes-KOH (pH 7.5) at 25 °C, 5 μM of FsPP was added to initiate the enzyme reaction. Because the reaction rate of using this alternative substrate was extremely slow, 40-μl portions of reaction mixture were withdrawn every 12 h and mixed with 10 mM EDTA to stop the enzyme reaction. The total time for assay was 36 h. The subsequent procedure to determine the reaction rate was the same as described above.

Production of UPPS Mutants—PCR technique was employed to produce UPPS mutants using our previously constructed plasmid as template, which contained the pET32Xa/LIC vector with insertion of the *E. coli Bos-12* UPPS gene (18). The mutagenic oligonucleotides for performing site-directed mutagenesis were 5′-GGCAATGGTCGCTTTGCAAAAAAGCAAGG-3′ for W31F (mismatched bases are underlined), 5′-AGTAGTGAAAACTTCAACCGACCAGCGCAG-3′ for W75F, 5′-TTTGTGTTCGCGCTAGAT-3′ for W91F, 5′-GGTGGACGTGCGGATATA-3′ for W149A, 5′-TTGCTTTTTCCAAATTGCC-3′ for W207F, and 5′-GATGTTCTCTTCCCCGAT-3′ for W221F. For the second PCR reaction, the forward primer 5′-GGTATTGAGGGTCGCATGTTGTCTGCT-3′ and reverse primer 5′-AGAGGAGAGTTAGAGCCATCAGGCTGT-3′ were used with the PCR products generated from the above mutagenic oligonucleotides to prepare mutant UPPS genes. Expression and purification of the mutant proteins were carried out as previously described (13).

Kinetic Constant Measurements of Mutant UPPS—The enzyme reaction was initiated by adding 0.01 μM mutant UPPS to a mixture containing various concentrations of FPP and [^{14}C]IPP. In the measurements of K_m and k_{cat} values of these mutant enzymes, five times the K_m value of one substrate was utilized to saturate enzyme, and concentrations of 0.5–5 K_m of the other substrate were used. All reactions were carried out in 100 mM Hepes-KOH buffer (pH 7.5), 50 M KCl, and 0.5 mM $MgCl_2$ at 25 °C in the presence of 0.1% Triton X-100. To measure the initial rate, portions of the reaction mixture were periodically withdrawn within 10% substrate depletion and mixed with 10 mM EDTA for reaction termination. The radiolabeled products were then extracted with 1-butanol and quantitated using a Beckman LS6500 scintillation counter. Data of initial rates *versus* substrate concentrations were analyzed by non-linear regression of the Michaelis-Menten equation (Equation 3) using the KaleidaGraph computer program (Synergy software) to obtain K_m and V_{max} values (19). The k_{cat} was calculated from V_{max}/[E].

$$v_o = V_{max}[\mathrm{S}]/(K_m + [\mathrm{S}]) \quad \text{(Eq. 3)}$$

where v_o is the initial velocity, [E] is the enzyme concentration, [S] is the substrate concentration, V_{max} is the maximum velocity, and K_m is the Michaelis constant.

Fluorescence Binding Experiments—The change of UPPS intrinsic fluorescence upon the addition of substrate was monitored using a F-4500 fluorescence spectrophotometer (Hitachi, Japan). The emission

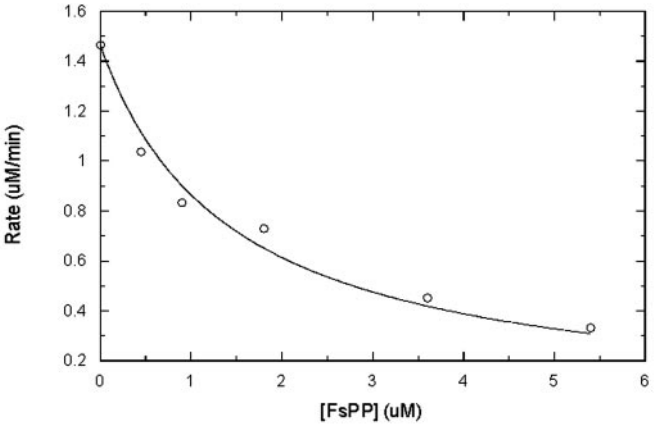

FIG. 2. **Inhibition of *E. coli* UPPS by (*S*)-farnesyl thiopyrophosphate.** The enzyme reactions with 0.03 μM enzyme, 3 μM FPP, and 50 μM [^{14}C]IPP were conducted in presence of various concentrations of inhibitor FsPP (0–6 μM). The reaction rate at each inhibitor concentration was determined by counting the radioactivity in the butanol layer (the reaction product). The plot of initial rate *versus* inhibitor concentration was used to determine the IC_{50} value of the inhibitor according to Equation 1 and 2.

TABLE I
Kinetic parameters of E. coli UPPS mutants with Trp replaced by Phe

UPPS	k_{cat}	K_m (FPP)	K_m (IPP)	Location of mutation
	s^{-1}	μM	μM	
Wild type	2.5 ± 0.1	0.4 ± 0.1	4.1 ± 0.3	
W31F	1.1 ± 0.1	2.0 ± 0.3	5.9 ± 0.8	α1
W75F	1.1 ± 0.1	1.8 ± 0.2	26 ± 3	Flexible loop
W91F	2.5 ± 0.1	0.4 ± 0.2	7.2 ± 1.3	α3
W149F	1.7 ± 0.1	0.7 ± 0.3	20 ± 4	α5
W207F	1.5 ± 0.1	3.4 ± 0.8	23 ± 3	Loop of βE-βF
W221F	3.5 ± 0.5	0.5 ± 0.04	14 ± 2	Loop of βF-α7

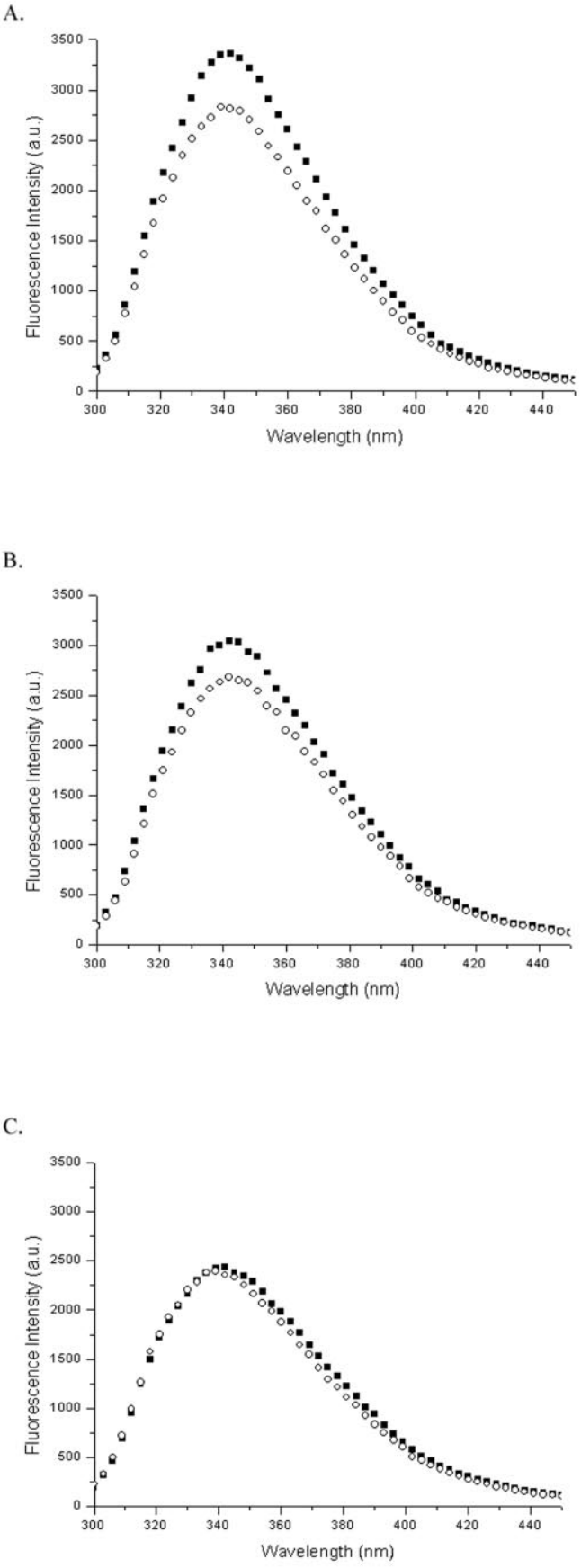

FIG. 3. **Quenching of UPPS fluorescence by the addition of FPP.** 15 μM FPP was added into the solution of 1 μM wild type enzyme and mutant UPPS in the presence of Mg^{2+}, and the fluorescence emission spectra from 300–450 nm were recorded. The fluorescence spectra of UPPS before and after the addition of FPP are shown with (■) and (○), respectively. Compared with the wild type UPPS as shown in *A*, W31F shows partially decreased fluorescence (*B*), whereas W91F has almost unchanged fluorescence upon addition of FPP (*C*). *a.u.*, absorbance units.

spectra were recorded from 300 to 450 nm upon excitation of wild-type and mutant UPPS at 285 nm. The fluorescence spectra of 1 μM UPPS in a buffer containing 100 mM Hepes-KOH (pH 7.5), 0.5 $MgCl_2$, and 50 mM KCl at 25 °C were measured before and after the addition of 15 μM FPP or FsPP. The experiments were also carried out in the absence of $MgCl_2$ to examine the role of the metal ion in FPP binding. For determination of the effect of IPP binding in the fluorescence spectra, the 1 μM enzyme (wild type or mutant) preincubated with 15 μM FsPP was mixed with 40 μM IPP in a buffer containing 100 mM Hepes-KOH (pH 7.5), 0.5 $MgCl_2$, and 50 mM KCl at 25 °C. The same experiment was also performed in the absence of $MgCl_2$.

Stopped-flow Experiments—Stopped-flow measurements were performed using an Applied Photophysics SX-18 MV stopped-flow spectrofluorimeter (Leatherhead, Surrey, UK). This apparatus has a 1.4-ms dead time, and the 1-cm path length was used. Protein Trp fluorescence emission above 320 nm was monitored using an excitation wavelength of 285 nm. A cut-off filter was used to prevent the detection of fluorescence signal below 320 nm. The observation cell was maintained at 25 °C during the stopped-flow measurements. The stopped-flow experiments were performed by mixing wild-type and mutant UPPS that is preincubated with FPP or FsPP with equal volumes of IPP solution in a buffer containing 100 mM Hepes-KOH (pH 7.5), 0.5 mM $MgCl_2$ and 50 mM KCl with IPP. The concentrations of enzyme, FPP or FsPP, and IPP cited in the text and in the parentheses are those after mixing, which are half the original concentrations due to an equal volume mixing. The apparent observed rate was obtained by fitting the stopped-flow trace (average of four repeated runs) with either a single exponential or a double exponential equation.

RESULTS

Synthesis of FPP Analogue FsPP—Initially we followed the published procedure for preparing geranyl thiopyrophosphate (16), which failed to yield FsPP at −35 °C probably due to the less reactive farnesyl chloride in the coupling reaction with thiopyrophosphate. By elevating the temperature to 25 °C, the desired product FsPP was obtained with the final yield of 70%. The synthesis of FsPP is outlined in Scheme 1. This substrate analogue was used in the inhibition studies, fluorescence binding, and stopped-flow experiments as described below.

FsPP Is an Inhibitor and an Alternative Substrate for UPPS—As shown in Fig. 2, the IC_{50} of the inhibitor in the presence of 0.03 μM enzyme, 3 μM FPP, and 50 μM IPP was ~1.3 ± 0.1 μM, which corresponds to 0.2 μM K_i value according to Equations 1 and 2. As expected, this substrate analogue binds to the enzyme with similar affinity as the substrate FPP (K_m = 0.4 μM). The FsPP also served as an alternative substrate for UPPS but with a much slower rate. The k_{cat} value measured at 25 °C was 3.1×10^{-7} s^{-1}, 10^7 times slower than the k_{cat} value of the enzyme reaction using FPP as the substrate.

Site-directed Mutagenesis and Kinetic Parameters of the Mutant UPPS—The UPPS mutants including W31F, W75F, W91F, W149F, W207F, and W221F were produced. These mutant enzymes were expressed as His-tag fusion proteins using *E. coli* BL21 as host cells under the control of a T7 promoter. The yield of each protein is ~100 mg/liter of culture. The protein was purified using the nickel nitrilotriacetic acid column, and the tag was cleaved by incubation with Factor Xa protease. The purity of the purified protein was >95%, judged by SDS-PAGE analysis (data not shown). As summarized in Table I, the kinetic parameter measurements reveal that W75F has larger FPP and IPP K_m values of 1.8 and 26 μM, respectively. W31F has an increased FPP K_m value (2 μM) without the change of k_{cat} and IPP K_m values. These results indicate that

Trp-31 and Trp-75 are part of the active site and involved in the substrate binding. W207F displays 6-fold larger IPP K_m value (23 μM) and an 8-fold increase FPP K_m value (3.4 μM), whereas its k_{cat} value is similar to that of the wild type. This residue is located at the interface of the UPPS dimer (Fig. 1*B*) and stacks with Arg-148 from the other subunit. W149F mutation also results in a five-times increased IPP K_m value (20 μM). Based on the K_m value measured for each mutant, sufficient quantity of substrate (at least 5-fold of K_m value) was used in the following experiments to saturate the enzyme.

FPP Quenches the UPPS Fluorescence—A fluorescence spectrophotometer was employed to monitor the change of protein intrinsic fluorescence upon adding the substrate. As shown in Fig. 3*A*, 15 μM FPP reduces the intrinsic fluorescence of 1 μM wild-type UPPS in the presence of Mg^{2+}. FPP still quenches the wild-type UPPS fluorescence in the absence of the metal ion, indicating that FPP binding to the enzyme does not require Mg^{2+} (data not shown). The fluorescence of mutant UPPS other than W31F and W91F is quenched by FPP with comparable magnitude to the wild-type UPPS (data not shown). In contrast, the fluorescence of 1 μM W31F is partially reduced (Fig. 3*B*), and that of W91F is almost not changed by adding 15 μM FPP to the protein (Fig. 3*C*). These indicate that when FPP is bound to the wild type UPPS, it mainly quenches the fluorescence of Trp-91.

IPP Increases the Fluorescence of Binary UPPS·FPP (FsPP) Complex—The addition of IPP to the UPPS solution in the absence of the other substrate FPP does not alter the protein fluorescence (data not shown). However, the addition of IPP to a preformed binary UPPS·FPP complex enhances fluorescence of the protein complex (data not shown). When the FsPP was used instead of FPP, the protein fluorescence also increases, indicating that the binding of IPP to the E·FsPP accounts for most of the protein fluorescence change (Fig. 4*A*). FsPP reduces the wild-type protein fluorescence as FPP does (Fig. 4*A* shows the fluorescence spectra of UPPS (■) and UPPS complexed with FsPP (○)), and the fluorescence increases to a higher level upon the addition of 40 μM IPP in the presence of Mg^{2+} (*asterisks*). On the other hand, FsPP still quenches the UPPS fluorescence, but the addition of IPP fails to increase the fluorescence of the complex in the absence of Mg^{2+} (Fig. 4*B*). This indicates that the metal ion is required for the binding of IPP to the UPPS complexed with FsPP.

Stopped-flow Experiments—Because there are changes of protein fluorescence by adding FPP into enzyme as well as IPP into the UPPS·FsPP (or UPPS·FPP) complex, the fluorescence stopped-flow method was used to measure the progress of these fluorescence changes in ways similar to previous studies (20, 21). In these experiments, the emission of the Trp fluorescence above 320 nm was monitored by excitation of the UPPS sample at 285 nm. No fluorescence change could be detected in the time scale (ms) of the stopped-flow instrument by mixing 1 μM enzyme with 5–15 μM FPP (data not shown) despite the observable fluorescence difference in the steady-state fluorescence spectra shown above. This indicates that the binding of FPP may be too fast to be measurable due to the small FPP K_m on our stopped-flow apparatus, which has a dead time of 1.4 ms. During the binding of IPP with the enzyme in the absence of FPP, no fluorescence change with time could be observed by mixing 1 μM enzyme and 5–40 μM IPP in the presence of 0.5 mM $MgCl_2$ (data not shown). This is not surprising since no net fluorescence difference could be detected between the spectrum of UPPS alone and that of the UPPS-IPP mixture. We then mixed by stopped-flow IPP (20 μM) with the enzyme (2.5 μM) that was preincubated with FPP (5 μM), since IPP enhances the fluorescence of the enzyme complex as shown in Fig. 4*A*. In this

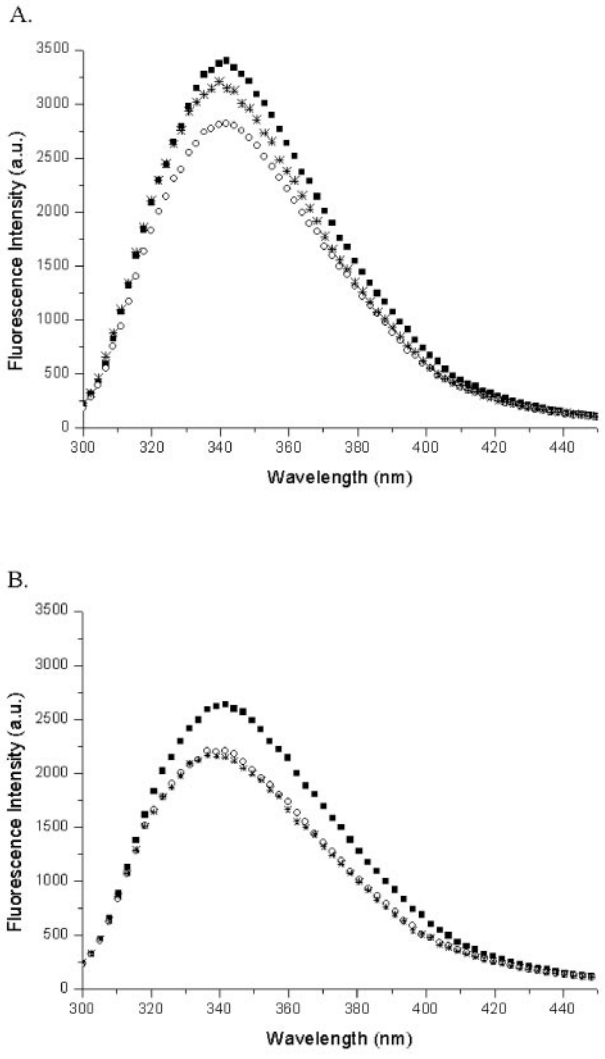

FIG. 4. **The enhancement of fluorescence upon the binding of IPP with UPPS and FsPP complex in the presence of Mg^{2+}.** The data represent the fluorescence spectra of UPPS (■), UPPS complexed with FsPP (○), and the addition of IPP to the complex (*asterisk*). The fluorescence of wild-type UPPS (1 μM) quenched by the addition of FsPP (15 μM) in the presence Mg^{2+} was enhanced by adding IPP (40 μM) as shown in *A*. On the other hand, the increase of fluorescence was not seen in the absence of Mg^{2+}, as shown in *B*.

stopped-flow experiment, the change of Trp fluorescence signal with time (a stopped-flow trace) was observed with three phases. The two slow phases observed in the 10-s window are shown in Fig. 5*A*. The fastest phase and part of the slow phase in the 200-ms window are shown in Fig. 5*B*. The data of Fig. 5*B* were fitted using a double exponential equation to obtain the rate constants of 95 and 6 s^{-1} for the first and the second phase, respectively. These data are complicated by the signals from both the binding of IPP to the complex and the subsequent enzyme reaction. To interpret these phases of the stopped-flow data, UPPS (2.5 μM) preincubated with FsPP inhibitor (5 μM) was used to mix with IPP (20 μM) in a stopped-flow experiment. This is shown in Fig. 5*C* as a quick increase of fluorescence, which plateaus within 20 ms with an observed rate of 90 s^{-1}. The observed rate is IPP concentration-dependent, indicating that it is resulted from the binding of IPP to the UPPS·FsPP complex. Measurements of the observed rate *versus* IPP concentration give a k_{on} value of 2 μM^{-1} s^{-1} for the IPP binding. FsPP did not react with IPP during this short period of time, and thus, the two slow phases were not seen in the 10-s time frame of the stopped-flow experiment in mixing IPP with the

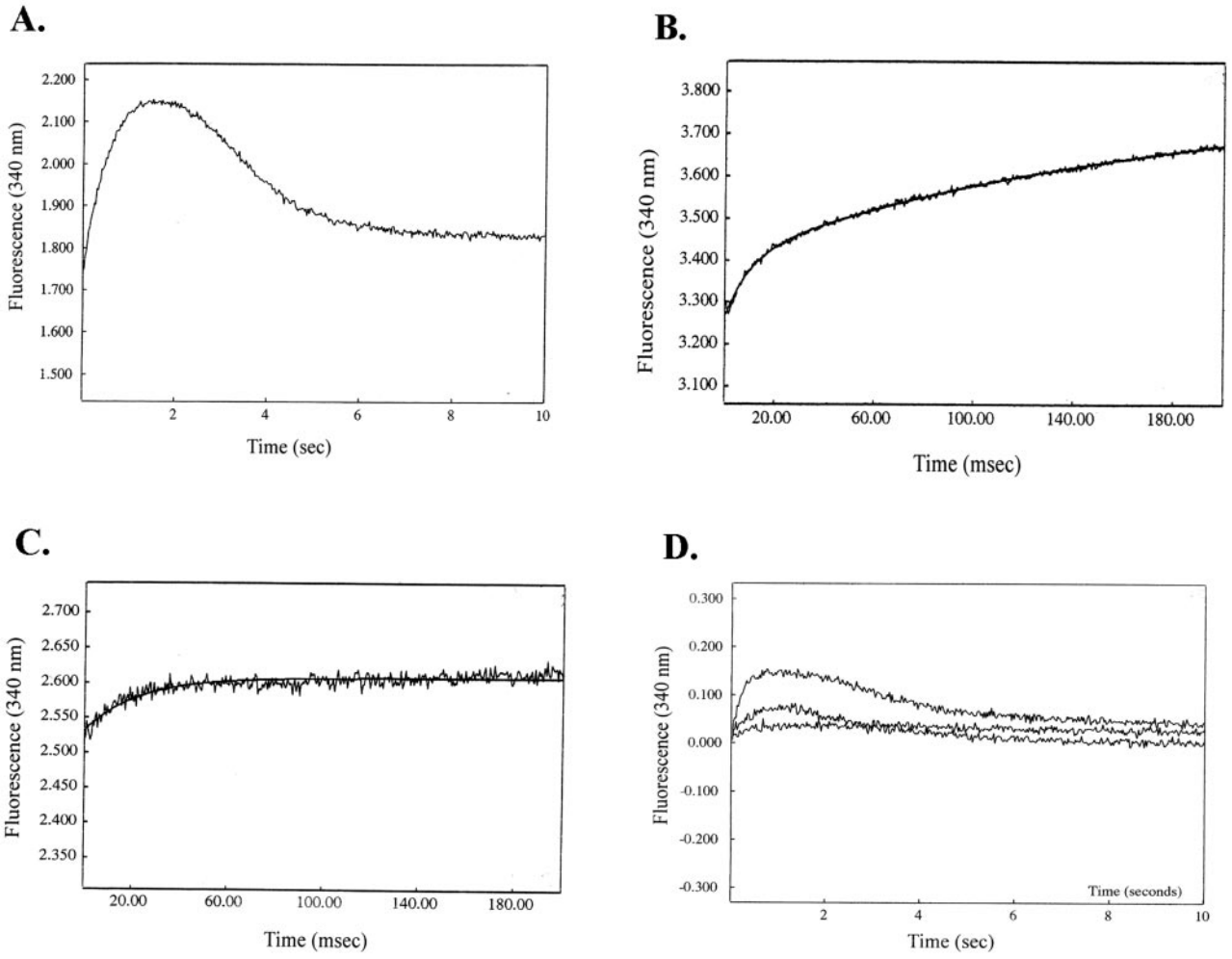

FIG. 5. **Stopped-flow experiments.** *A*, the binding of IPP to E·FPP monitored by the stopped-flow instrument. The fluorescence change with time in a mixed solution of enzyme (2.5 μM) preincubated with FPP (5 μM) and IPP (20 μM) was recorded. *B*, the 200-ms time window of the same stopped-flow experiment as in *A*, to show the fast phase. *C*, stopped-flow trace for the ternary complex formation of IPP with UPPS·FsPP. In this stopped-flow experiment, IPP (20 μM) was mixed with equal volume of enzyme solution (2.5 μM) preincubated with inhibitor FsPP (5 μM), and a fast binding signal with small amplitude was observed. *D*, the reduced amplitude observed for stopped-flow traces of the W149F and W207F in using 1 μM enzyme, 10 μM FPP, and 50 μM IPP. The data from the top to the bottom in the fluorescence-increasing phase are those for wild type, W149F, and W207F UPPS.

E·FsPP complex. Apparently, the two slow phases observed in mixing the UPPS·FPP complex with IPP are due to the protein conformational changes related to enzyme reaction and/or product release.

The stopped-flow measurements using the six UPPS mutants were performed. In these experiments, IPP (50 μM) was mixed with enzyme (1 μM) preincubated with FPP (10 μM) in the presence of 0.5 mM Mg^{2+}. Under this condition, W149F and W207F were found to show smaller but not zero amplitude for the stopped-flow signal compared with the wild-type enzyme (Fig. 5*D*). These two Trp residues together may account for the fluorescence change observed in the stopped-flow experiments for the wild-type UPPS. Other mutants, W31F, W75F, W91F, and W221F, gave a comparative level of stopped-flow trace with that of the wild-type UPPS (data not shown).

DISCUSSION

According to the crystal structure of UPPS, FPP was proposed to bind to the enzyme with its pyrophosphate group near the Asp-26, Asn-28, Arg-30, and Glu-198 area (11, 12). The present site-directed mutagenesis studies demonstrate that Trp-31 is involved in the FPP binding, probably through its hydrophobic interaction with the C_{15} carbon chain of FPP. W31F has a 5-fold larger FPP K_m value without significant changes of IPP K_m and k_{cat} values. As indicated by our fluorescence quenching studies, the addition of FPP partially quenches the Trp-31 fluorescence, consistent with the fact that Trp-31 is related to FPP binding. On the other hand, W91F exhibited almost no change in the fluorescence upon the addition of FPP. Trp-91 is located in the α3 helix, which kinks to a larger degree when a hydrophobic molecule occupies the active site, as demonstrated in our *E. coli* UPPS structure (Fig. 1*A*). From the above data, it is mainly the Trp-91 fluorescence, which is quenched by adding FPP to the wild type UPPS. The binding of FPP may relocate the α3 helix toward the active site via the movement of the flexible loop 72–83.

The quenching of fluorescence by FPP still occurs in the absence of Mg^{2+}, indicating that FPP binding may not require Mg^{2+}. This is consistent with our previous observation that the D26A mutation did not change the FPP K_m value (13). Previously, Asp-26 has been proposed to provide its carboxylate group for binding with FPP via Mg^{2+} (11). We suggest that the tight FPP binding may result from the simultaneous contributions of several amino acid residues in the active site, especially hydrophobic residues such as Trp-75 and Trp-31, as indicated by the site-directed mutagenesis studies presented here.

On the other hand, the binding of IPP absolutely requires the

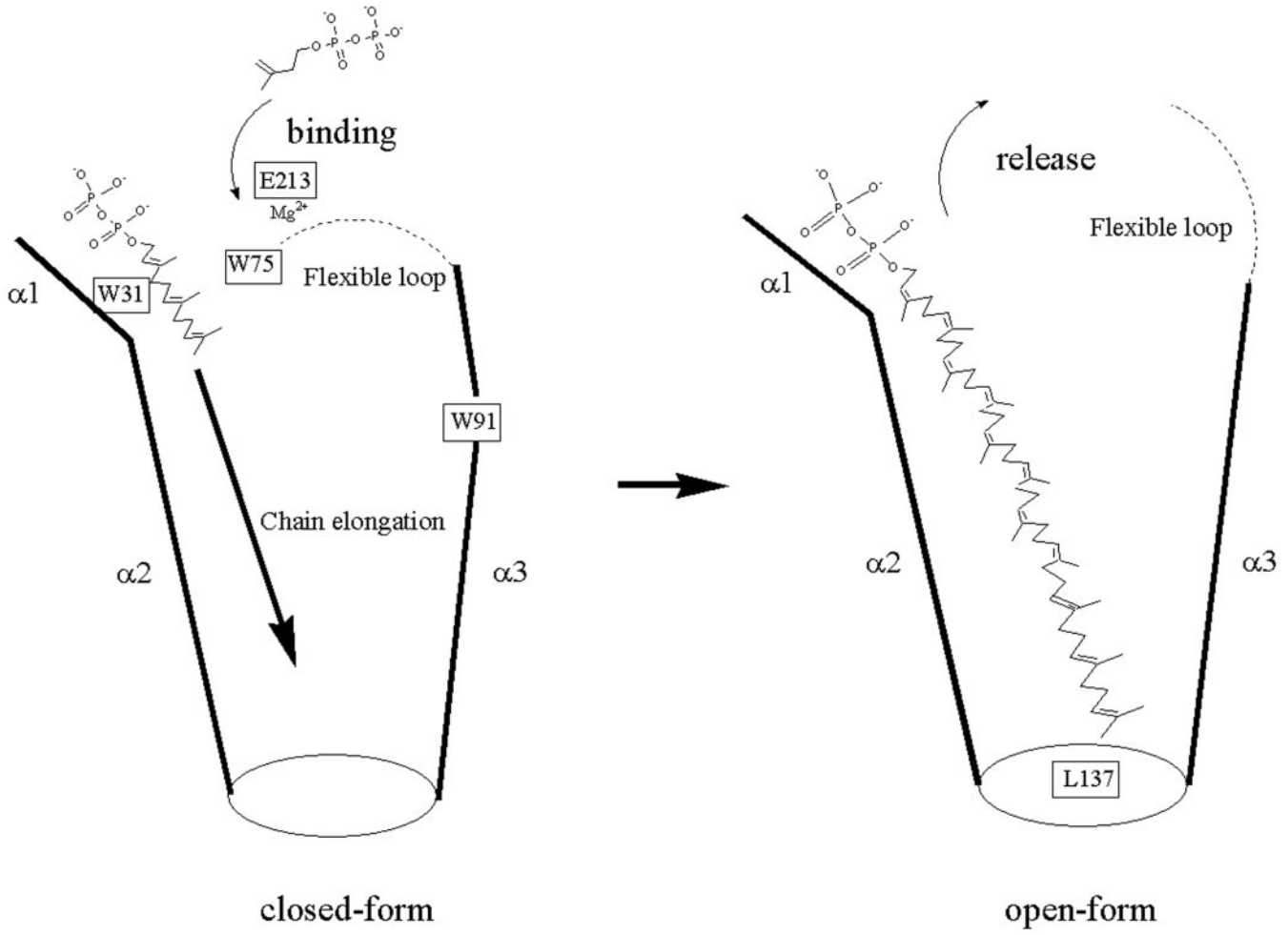

FIG. 6. **A model showing the inter-conversion of the closed and the open form of UPPS during substrate binding and product release.** Trp-31 is involved in the FPP binding, and Trp-75 is located in a loop that moves toward the active site upon the binding of FPP. The binding of IPP to the E·FPP triggers the binding phase (first phase) and subsequent conformation change for the enzyme reaction (second phase) and product release (third phase).

Mg^{2+} ion, as suggested by our data. IPP is proposed to bind to the site of Glu-213, which could employ its carboxylate group for the binding with Mg^{2+}-IPP. The mutant E213A has significantly reduced IPP affinity, as indicated by its markedly increased IPP K_m value (13).

According to our stopped-flow fluorescence studies, the IPP binding to the preformed complex of UPPS·FPP triggers the enzyme reaction with a three-phased fluorescence change; the first phase is due to the IPP binding, whereas the second and third phases are related to the enzyme reaction and product release. The intrinsic fluorescence of Trp-149 and Trp-207 residues likely contributes to these stopped-flow signals. Based on the crystal structure, Trp-207 and Trp-149 are located closely at the dimeric interface of UPPS. The side chain of Trp-207 is stacked with that of Arg-148 (next to Trp-149) from the other subunit. The conformational change during the enzyme catalysis represents a major one since it changes the fluorescence of the residues located in the dimer interface. Accordingly, the UPPS structure is flexible to allow the enzyme to catalyze multiple IPP condensations and the large product to exit the active site.

In the UPPS reaction, a single FPP reacts with eight molecules of IPP for product generation. It is reasonable to assume that FPP binds the enzyme first followed by the binding of IPP. Our fluorescence quenching data indicate that FPP could bind UPPS in the absence of IPP. However, the addition of IPP alone to the enzyme fails to produce fluorescence change unless FPP (or FsPP) is preincubated with the enzyme. These results are consistent with the assumption that the binding order is FPP first, followed by IPP.

The time scale of the protein conformational change measured by the stopped-flow apparatus seems consistent with the time course of the rate-limiting IPP condensation reaction for the conversion of C_{15} FPP to C_{55} UPP and further extension to C_{75}. In this time course, the C_{55} product is formed in about 2 s, and then the C_{60} to C_{75} products are generated within 10 s (*see Fig. 2B the supporting information of Ref. 18*). The stopped-flow trace increases in 2 s and then decreases by the end of 10 s (Fig. 5). Compared with the single-turnover time course data (18), the two slow phases observed in the stopped-flow experiment may represent the conversion of C_{15} to C_{55} reaction in the active site and the product release, respectively. The product release process is accompanied with the conversion of C_{55} to the extended length of C_{75} due to the slow product release in the absence of Triton (18). Thus, the increased fluorescence due to the substrate binding and the subsequent reaction might cause the formation of a "closed-form" UPPS, which provides a better interaction between the enzyme with the substrates and the intermediates. After the reaction, decreased fluorescence represents the shift of UPPS structure to an "open form" for the product release triggered by the crowding prenyl chain of the product since the bottom of the tunnel is sealed by the large amino acid residue Leu-137 (12). This model is shown in Fig. 6.

Our stopped-flow data provide an insight of the *E. coli* UPP reaction mechanism and reveal a novel intrinsic protein fluo-

rescence change associated with the substrate binding, subsequent reaction, and product release. These fluorescent properties of UPPS in conjunction with previous site-directed mutagenesis and crystallographic studies allow the identification of the substrate binding site and measurements of IPP binding and reaction rates to be made. Furthermore, stopped-flow technology could be used as an alternative method of enzyme activity assay to the current way of using radiolabeled IPP. Therefore, this technology may be potentially useful in the search of enzyme inhibitor that could serve as broad spectrum of antibacterial agent since UPPS enzyme is essential in bacterial survival.

Acknowledgment—We thank Dr. T. P. Ko for preparing Fig. 1.

REFERENCES

1. Ogura, K., Koyama, T., and Sagami, H. (1997) *Subcell. Biochem.* **28,** 57–87
2. Ogura, K., and Koyama, T. (1998) *Chem. Rev.* **98,** 1263–1276
3. Allen, C. M. (1985) *Method Enzymol.* **110,** 281–299
4. Shimizu, N., Koyama, T., and Ogura, K. (1998) *J. Biol. Chem.* **273,** 19476–19481
5. Sato, M., Sato, K., Nishikawa, S. I., Hirata, A., Kato, J. I., and Nakano, A. (1999) *Mol. Cell. Biol.* **19,** 471–483
6. Schulbach, M. C., Brennan, P. J., and Crick, D. C. (2000) *J. Biol. Chem.* **275,** 22876–22881
7. Oh, S. K., Han, K. H., Ryu, S. B., and Kang, H. (2000) *J. Biol. Chem.* **275,** 18482–18488
8. Robyt, J. (1998) in *Essentials of Carbohydrate Chemistry*, pp. 305–318, Springer-Verlag, New York
9. Hussey, H., and Baddiley, J. (1976) in *The Enzymes in Biological Membranes*, Vol. 2, pp. 227, Plenum Press, New York
10. Apfel, C. M., Takacs, B., Fountoulakis, M., Stieger, M., and Keck, W. (1999) *J. Bacteriol.* **181,** 483–492
11. Fujihashi, M., Zhang, Y.-W., Higuchi, Y., Li, X.-Y., Koyama, T., and Miki, K. (2001) *Proc. Natl. Acad. Sci. U. S. A.* **98,** 4337–4342
12. Ko, T. P., Chen, Y. K., Robinson, H., Tsai, P. C., Gao, Y.-G., Chen, A. P.-C., Wang, A. H.-J., and Liang, P. H. (2001) *J. Biol. Chem.* **276,** 47474–47482
13. Pan, J. J., Yang, L. W., and Liang, P. H. (2000) *Biochemistry* **39,** 13856–13861
14. Kharel, Y., Zhang, Y.-W., Fujihashi, M., Miki, K., and Koyama, T. (2001) *J. Biol. Chem.* **276,** 28459–28464
15. Fujikura, K., Zhang, Y.-W., Yoshizaki, H., Nishino, T., and Koyama, T. (2000) *J. Biochem.* **128,** 917–922
16. Phan, R. M., and Poulter, C. D. (2000) *Org. Lett.* **2,** 2287–2289
17. Segel, I. H. (1993) in *Enzyme Kinetics: Behavior and Analysis of Rapid Equilibrium and Steady-state Enzyme Systems* (Wiley Classics Library, ed) pp. 100–118, John Wiley & Sons, Inc., New York
18. Pan, J. J., Chiou, S. T., and Liang, P. H. (2000) *Biochemistry* **39,** 10936–10942
19. Fersht, A. (1984) in *Enzyme Structure and Mechanism* pp. 99–101, W. H. Freeman and Co., New York
20. Liang, P. H., and Anderson, K. S. (1998) *Biochemistry* **37,** 12206–12212
21. Liang, P. H., and Anderson, K. S. (1998) *Biochemistry* **37,** 12195–12205
22. Kraulis, P. J. (1991) *J. Appl. Crystallogr.* **24,** 946–950